2022
9(1), 61-67

Journal of
MATERIALS NANOSCIENCE

p-Co_3O_4 supported heterojunction Carbon Nanofibers for Ammonia gas sensor applications

Ramakrishnan Vishnuraj, Rajesh Unnathpadi, Biji Pullithadathil*

Nanosensor Laboratory, PSG Institute of Advanced Studies, Coimbatore-641004, INDIA.

Submitted on: 17-Nov-2021 Accepted and Published on: 15-Feb-2022

Article

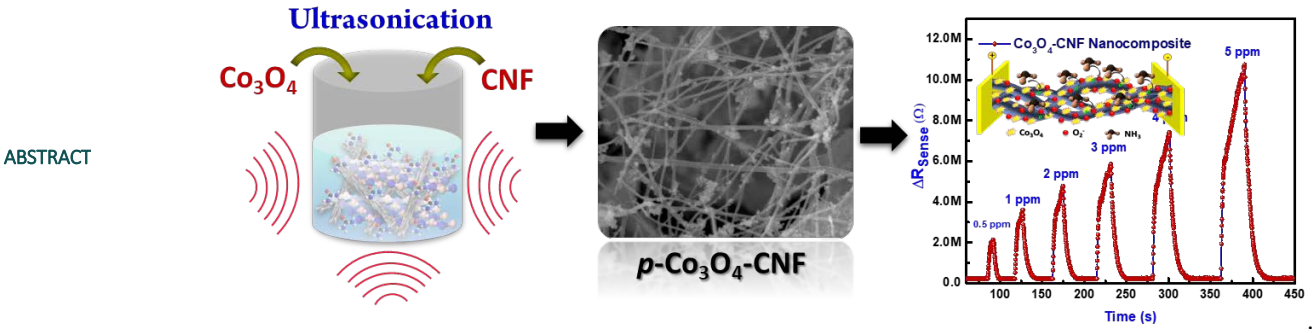

ABSTRACT

Trace level detection of gaseous ammonia is extremely important both in terms of environmental monitoring as well as health monitoring sectors. Metal oxide semiconductor, *p*-Co_3O_4 based nanostructures have been widely used as gas sensing materials to detect a wide range of toxic gases. However, the pristine *p*-Co_3O_4 based sensors always face poor sensitivity and selectivity towards target gases. In order to enhance the sensitivity and selectivity of *p*-Co_3O_4 based NH_3 sensors, integration into carbon nanofibers forming heterojunction materials could be a suitable strategy. Herein, we report the synthesis and characterization of NH_3 gas sensing characteristics of *p*-Co_3O_4 supported heterojunction carbon nanofibers (CNF) for the detection of trace level concentration of NH_3. Structural and morphological characterization of the material have been carried out using X-ray diffraction (XRD), Raman spectroscopy and Field-Emission Scanning Electron microscope (FE-SEM). The evaluation of gas sensing properties of *p*-Co_3O_4 supported CNFs exhibited high sensitivity for detecting NH_3 at lower working temperature and plausible gas sensing mechanism has been discussed. This study can pave the way to novel strategies for developing and commercialize low-cost, highly sensitive NH_3 sensors application.

Keywords: *p-Co₃O₄, Carbon Nanofibers, room temperature NH₃ gas sensor, sensing mechanism*

INTRODUCTION

Recently, there has been a significant increase in the demand for air pollution monitoring and control, in which ammonia is being one of the most prominent pollutants generating serious environmental issues.[1,2] Since ammonia is being using in several fields such as agriculture, cleaning products, refrigerants, etc., because it can cause serious health concerns, it necessitates stringent safety procedures and also higher concentration of NH_3 leads to combustible in the presence of air at 50°C.[3,4] Hence, it is highly desirable to develop cost-effective high-performance sensor material to detect trace level concentration of NH_3 in the environment. In various industries, such as automotive, industrial process monitoring, medical diagnostics, air quality management and solid state based chemical sensors finds their applications in detection of trace level concentrations of NH_3 in environment.[5,6] Metal oxide based chemiresistive type sensors generally utilizes least expensive sensor materials such as, SnO_2, ZnO, CuO, NiO, In_2O_3, WO_3, Co_3O_4 etc.[7–11]

Based on the conductivity of the semiconductor-based sensor materials, *p*-type metal-oxide semiconductors are less explored than *n*-type MOS materials which are in the early stages of development.[12,13] In comparison to *n*-type metal oxides, *p*-type metal oxides have demonstrated superior performance in gas detection due to the majority of hole carriers, their charge transport, resistance towards humidity upon gas exposure, enhanced catalyst properties, long-standing stability, and lower open circuit resistance.[14,15] Among various *p*-type metal-oxide semiconductors, cobalt oxide (Co_3O_4) has gained a great attention towards detection of NH_3 based on various type of transduction mechanisms because of its corrosion resistance, incredible sensitivity, response/recovery, and stability even at ambient condition with improved electrical and chemical properties as

*Corresponding Author: Dr. P. Biji, Associate Professor in Nanotechnology, PSG Institute of Advanced Studies, Peelamedu, Coimbatore-641004, INDIA
Tel: +91 422 4344000, Ext: 4541
Email: biuja123@yahoo.co.in; pbm@psgias.ac.in

URN:NBN:sciencein.jmns.2022.v9.289

ISSN: 2394-0867
https://pubs.thesciencein.org/jmns

well as their abundance.[16,17] However, pristine Co_3O_4 does not provide any adequate sensor response to NH_3, particularly under ambient conditions. Therefore, it is necessary to modify pristine Co_3O_4 by integration with suitable materials to form heterojunctions to enhance the sensor performance.

In this scenario, it is established that the physical and chemical properties of heterojunction nanostructures are greatly influenced by their dimensionality, size, and morphology. In order to modify the properties of Co_3O_4, it could be functionalized on conducting carbon-based nanostructures which can exhibit improved NH_3 sensing performance.[18,19] Carbon-based nanomaterials can impose remarkable sensor response to varied gaseous molecules under ambient conditions, owing to its magnificent surface to volume ratio and relatively high electrical conductivity.[20] Among various carbon nanostructures, carbon nanofibers are considered as an attractive support material for many applications due to its unique one-dimensional structure that exhibit high aspect ratio, low density and high electrical conductivity.[21] Therefore, adopting carbon nanofibers as a suitable support material to form MOS heterojunctions could be a unique strategy to further increase the NH_3 sensing performance due to its fast charge transport mechanism which has not been explored widely.[22,23]

In this investigation, we have synthesized *p*-Co_3O_4 supported heterojunction carbon nano-fibers using simple ultrasound probe-sonication process. The pristine and heterojunction materials have been characterized using spectroscopic and microscopic analysis which confirmed the formation of heterojunction nanofibers and a uniform distribution of *p*-Co_3O_4 nanoparticles on the surface of carbon nanofibers was achieved. NH_3 gas sensing properties of *p*-Co_3O_4 supported heterojunction carbon nano-fibers revealed enhanced sensor response under ambient conditions compared to pristine *p*-Co_3O_4 nanoparticles. The gas sensing mechanism of heterojunction nanocomposite during NH_3 exposure also has been discussed.

EXPERIMENTAL PROCEDURE

Chemicals Used: Cobalt Nitrate ($Co(NO_3)_2.H_2O$, 99.8%, Merck), potassium nitrite (KNO_2, 99.8%, Merck), Acetic acid (CH_3COOH, 99.8%, Merck), Sodium hydroxide (NaOH, 99.8%, Merck), ethanol (C_2H_5OH, 99%, Merck), Sulfuric acid (H_2SO_4, Merck) and Nitric acid (HNO_3, Merck) Polyacrylonitrile (PAN, 150,000 g/mol), Dimethyl formamide (C_3H_7NO, 99%, Merck), were used without any further purifications. Deionised ultra-pure water was used throughout the experiments.

Synthesis of *p*-Co_3O_4 nanoparticles

p-Co_3O_4 nanoparticles were synthesized by simple wet chemical hydrothermal synthesis method. Typically, in 1 wt% of cobalt nitrate solution, 0.5:4 ratio of potassium nitrate and acetic acid was blended and kept stirring for 15 min. After complete dissolution of the substances, 2 M sodium hydroxide was slowly added to the above solution. Stirring was continued for another 15 min and the obtained mixture was transferred and sealed in a 100 mLTeflon lined stainless steel autoclave. The autoclave was maintained at a temperature of 180ºC for 12 h. After the hydrothermal process, the solution was cooled to ambient condition and the obtained powder sample was purified with a mixture of ethanol and DI water and kept in oven at 80ºC for drying.[24,25]

Synthesis of Carbon nanofibers:

Carbon nanofibers (CNF) were synthesized using electrospinning method. For this, Polyacrylonitrile (PAN) was dissolved in Dimethyl formamide (8 wt %) stirred for 2hr at 60ºC. The needle and the collector were separated with a distance of 21cm and applied high voltage of 20 kV was employed for Electrospinning. The PAN loaded syringe was maintained a constant flow rate of 0.1mL/h. The obtained polymeric mat on the copper foil was further converted to CNFs by thermal processing. Stabilization of the mat at 300°C in air was followed by carbonization at 800°C in N_2 atmosphere with a heating rate of 3°C/min. Further to synthesis the heterojunction nanocomposite, CNFs were acid functionalized by treating with nitrating mixture (H_2SO_4 and HNO_3).[26]

Synthesis of *p*-Co_3O_4 nanoparticles supported Carbon nanofiber:

p-Co_3O_4 nanoparticles supported heterojunction Carbon nanofiber was synthesized using simple probe-sonication process. The functionalized CNFs were dispersed in the ethanol solution and simultaneously an appropriate amount of as synthesized *p*-Co_3O_4 nanoparticles was added to this solution. The sample was sonicated using a high frequency probe-sonication which was maintained at 20 kHz for 30 min with time interval of 2 min. The collected precipitate sample was filtered and washed using ethanol and DI water and finally dried at 60ºC overnight.

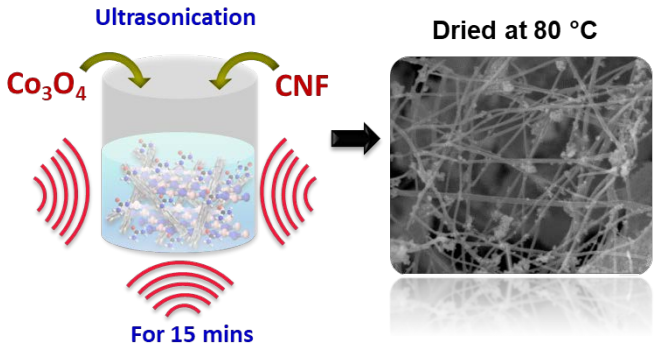

Scheme 1. Synthesis of *p*-Co_3O_4 supported heterojunction carbon nano-fibers.

Evaluation of dynamic NH_3 gas sensing procedure:

The sensor device was fabricated as inter-digitated array (IDA) electrode made of Au (~200 nm) with an inter finger gap of 16 µm using planar DC magnetron sputtering on alumina substrates. Thin films of pure *p*-Co_3O_4 nanoparticles and *p*-Co_3O_4 supported heterojunction carbon fibers (1 mg/mL) were dispersed in ethanol and drop-casted on IDA transducer electrodes at 60ºC. The gas sensing properties of the materials were analyzed using a custom-built gas sensor test station consisting of a stainless-steel double-walled test chamber equipped with temperature-controlled hot

stage, sensor holder, mass flow controllers (MFC, Alicat, USA), digital multimeter (Agilent 34401A, USA) connected with a data acquisition system interfaced with Labview software. A temperature controller (Eurotherm, 2420, U.K.) was used to maintain the working temperature of the sensor mounted inside the sensing chamber. The required concentration of a NH_3 gas in the chamber was attained by introducing a derived quantity of NH_3 gas mixed with carrier gas (high pure Nitrogen (N_2), 99.999%) using Owlstone gas generator unit (OVG-4, U.K.). The gas concentration was accurately controlled using OVG gas generator with pre-calibrated permeation tubes with a constant flow rate of 300 sccm was maintained throughout the experiment.

Results and Discussion

In this investigation, *p*-Co_3O_4 nanoparticles supported heterojunction carbon nanofibers were synthesized using ultrasound high frequency probe-sonication method. The carbon nanofibers were surface activated via acid functionalization for effective formation of heterojunction. During high frequency irradiation, the dispersed *p*-Co_3O_4 nanoparticles tends to be anchored over the active sites of acid functionalized carbon nanofiber surface. The *p*-Co_3O_4 nanoparticles maintained a strong bonding with the carbon nanofibers forming nanocomposite heterojunctions as depicted in scheme 1.

Structural and morphological characterization:

The structural analysis of pristine *p*-Co_3O_4 nanoparticles and *p*-Co_3O_4 supported heterojunction carbon nano-fibers has been studies using X-ray diffraction pattern as shown in Figure 1. The high intense, prominent peaks observed from the XRD pattern of pristine *p*-Co_3O_4 nanoparticles and *p*-Co_3O_4 supported heterojunction carbon fibers reveals the crystalline structure of the samples. The major diffraction peaks arise at the 2-theta values of 19°, 25.4°, 31.6°, 37.3°, 39.2°, 44.7°, 55.6°, 59.4°, 62.9° and corresponding to the (111), (220), (222), (311), (400), (422), (333), and (440) planes of respectively which represents the characteristic cubic crystal plane of Co_3O_4 confirmed from JCPDS file No: 43-1003.[27] The intense peak at 24.6° appeared for carbon nano-fibers is attributed to the amorphous graphitic

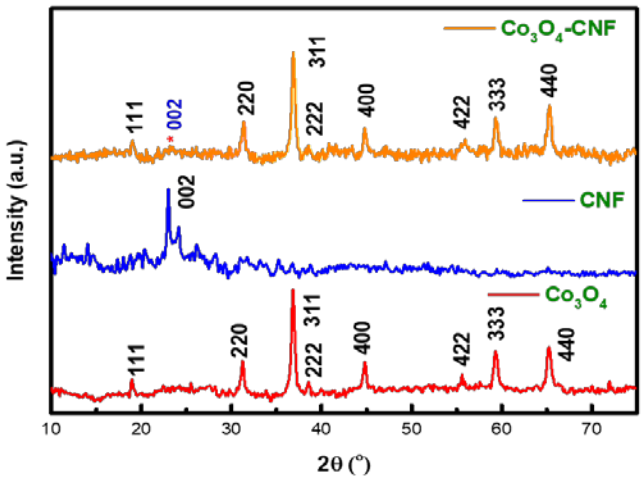

Figure 1. XRD patterns of *p*-Co_3O_4, carbon nano-fibers, and *p*-Co_3O_4 supported heterojunction carbon fibers

carbon with (002) plane present in the XRD pattern of carbon nano-fibers which is allotted to hexagonal graphite confirmed from the JCPDS card 41-1487 as depicted in Figure 1.[28] Further, XRD pattern of *p*-Co_3O_4 supported heterojunction carbon fibers shows the characteristics peaks of *p*-Co_3O_4 along with carbon nano-fibers features which further confirm the formation of effective heterojunctions without any impurities. There were no peak shifts or peak broadening observed.

The micro-Raman spectra acquired for Co_3O_4, CNFs, and *p*-Co_3O_4 supported heterojunction carbon fibers (Figure 2) was implemented to reveal the chemical identification through vibration modes of the composite material. The D and G bands of carbon nano-fibers and *p*-Co_3O_4 supported heterojunction carbon fibers are spotted at 963 and 937 cm^{-1}, and 652 and 644 cm^{-1} respectively, which is the breathing mode of the A_{1g} symmetry of defects with the presence of sp^3 carbon atom and the E_{2g} phonon mode of sp^2 carbon.[29] The I_D/I_G ratio was found to be decreased (1.01) for Co_3O_4 supported heterojunction carbon fibers compared to bare carbon fibers (1.02), assigning to the structural distortions caused by the interaction between Co_3O_4 nanoparticles with the carbon fibers. Raman peaks located at around 220, 464, 508, 602 and 669 cm^{-1}, corresponding to F_{2g}, E_g, F_{2g1}, A_{1g}, F_{2g2} vibrational modes of Co_3O_4.[30] The Raman peaks of *p*-Co_3O_4 supported heterojunction carbon fibers exhibited characteristic vibration modes of both Co_3O_4 and carbon nano-fibers confirming the presence of Co_3O_4 nanoparticles anchored over the carbon nano-fibers forming heterojunctions. [31]

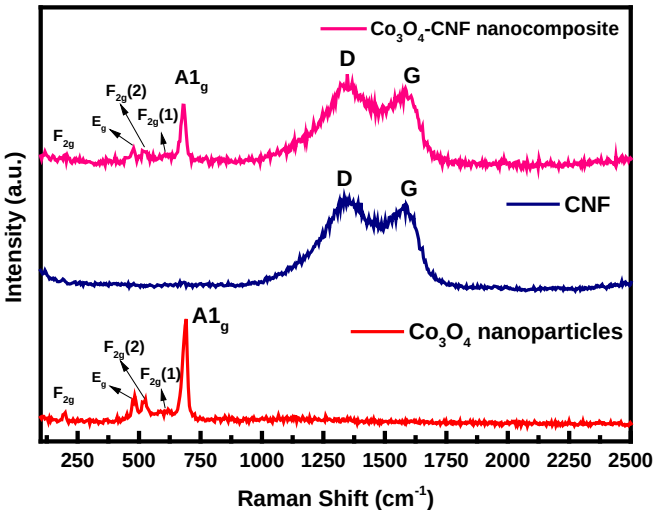

Figure 2. Raman Spectra of *p*-Co_3O_4, carbon nano-fibers, and *p*-Co_3O_4 supported heterojunction carbon fibers

In order to study the morphological characteristics of Co_3O_4, CNFs, and *p*-Co_3O_4 supported heterojunction carbon fibers, SEM analysis was carried out to as shown in Figure 3(A-D). The dispersed Co_3O_4 nanoparticles shows the particles size of 85 ± 10 nm without agglomeration and SEM image of carbon nano-fibers depict the fiber diameter of 150 ± 15 nm with several length of micrometer as shown in Figure 3 (A-B). The heterojunction material depicted the attachments of Co_3O_4 nanoparticles all over

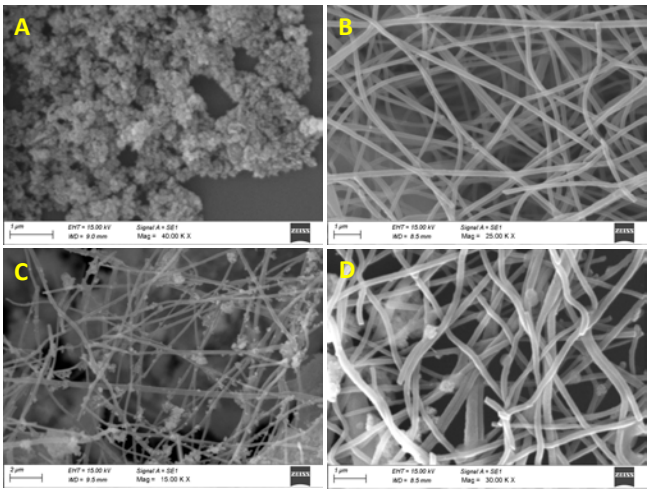

Figure 3. SEM images of the (A) Co_3O_4 NPs, (B) carbon nano-fibers, (C-D) *p*-Co_3O_4 supported heterojunction carbon nano-fibers.

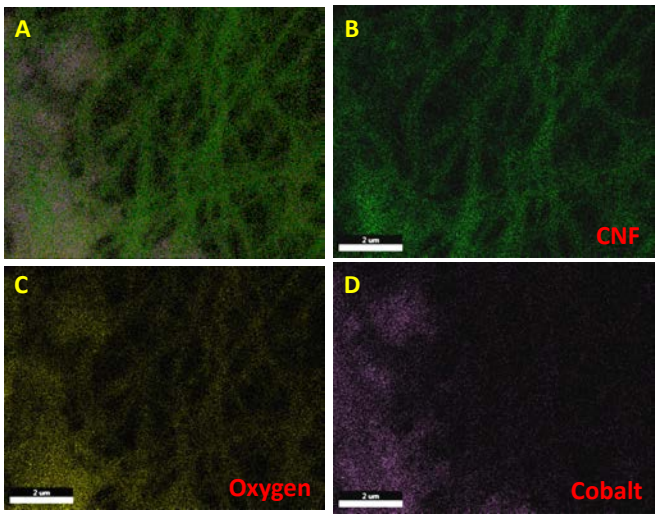

Figure 4(A-D) Corresponding EDS Elemental mapping of *p*-Co_3O_4 supported heterojunction carbon nano-fibers

the region of carbon nano-fibers which is evident from Figure 3(C-D). The corresponding EDX spectra show the presence of Co, O, and C elements as depicted in Figure S1. Further, EDX mapping clearly implies the presence of Co and O elements over the carbon nano-fibers as shown in Figure 4(A-D) which confirms the formation of *p*-Co_3O_4 supported heterojunction carbon fibers.[22,32]

Gas sensing Properties of Co3O4 NPs and p-Co3O4 supported carbon nanofibers:

NH_3 gas sensing properties of Co_3O_4 NPs and *p*-Co_3O_4 supported heterojunction carbon nano-fibers were evaluated using an in-house sensor test station developed in our laboratory. Since both the pristine and heterojunction sensor materials operate in room temperature, the sensor calibration towards NH_3 gas was carried out in the ambient condition. Dynamic response and recovery graph of Co_3O_4 NPs shows increased resistance change when exposure to NH_3 gas, in related with the usual behavior of *p*-type MOS interact with reducing gas evident in the Figure 5(A&D).[33,34] During the evaluation of sensor response, NH_3 gas was purged with N_2 as carrier gas after achieving the steady baseline. The change in increasing resistance rapidly to a saturation after exposure to NH_3 and resistance decreases to the base resistance once the flow of NH_3 gas was stopped. The relative sensor response ($\Delta R/R_a$) versus concentration ranging from 500 ppb to 5 ppm was monitored and shown in Figure 5(B&E). The NH_3 sensor properties were tabulated in Table S1. The sensitivity rapidly amplified from ~3.6% to ~45% for 500

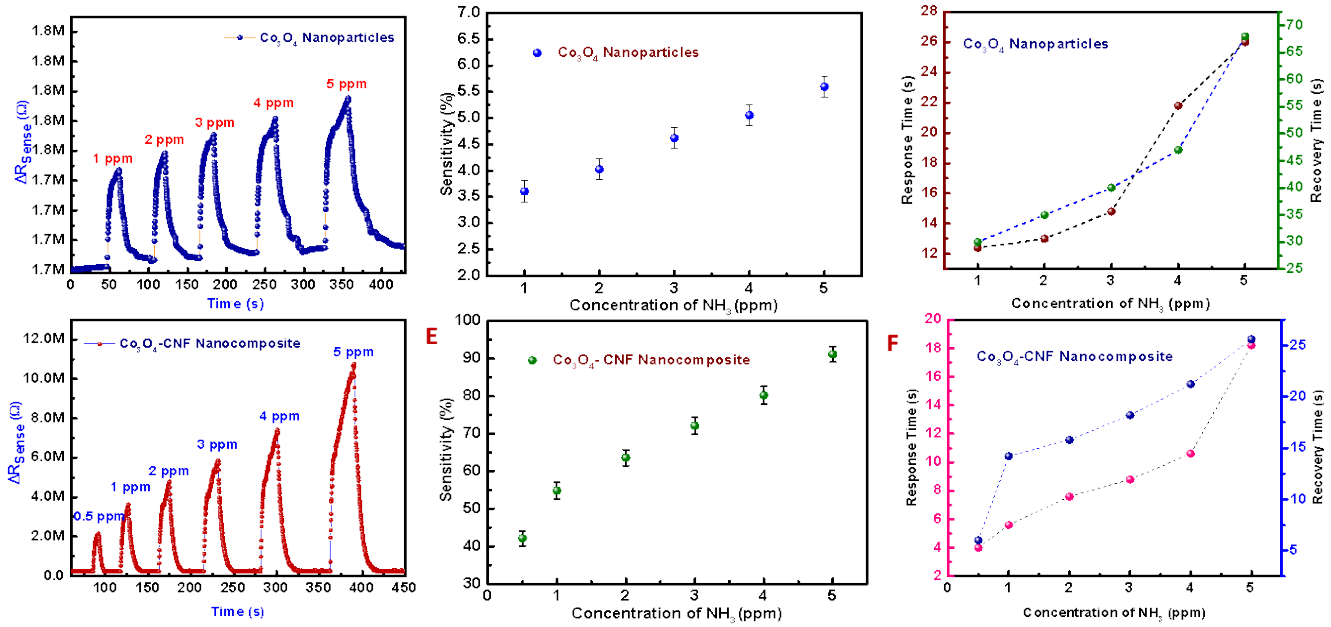

Figure 5. Dynamic NH_3 sensing characteristics of (A) Co_3O_4 NPs and (B) *p*-Co_3O_4 supported heterojunction carbon fibers, (B & E) NH_3 response as a function of concentration, (C & F) NH_3 response as a function of response and recovery time.

Table 1. Comparison of the NH_3 sensing characteristics of *p*-Co_3O_4 supported heterojunction carbon nano-fibers based sensors reported in the literature with the present sensor.

Sensor materials	Fabrication method	Measuring range (ppm)	Operating temp.	Response (Rg/Ra)	T_{Res}/T_{Rec}(s)	Ref.
Nano-sheet Co_3O_4 arrays	Hydrothermal-method	0.2-100 ppm	RT	2.3@20 ppm	9/134	[11]
Co_3O_4 Nanorods	Hydrothermal Strategy	10–200 ppm	160ºC	3.0@10 ppm	2/4	[36]
Co_3O_4/SnO_2 Nanospheres	Hydrothermal Process	10–100 ppm	200ºC	2.8@10 ppm	4/17	[37]
Co_3O_4@CuO Nanochains	Electrospinning	1–100 ppm	RT	5.72@100 ppm	1.3/31.3	[33]
rGO-Co_3O_4 Nanofibers	Electrospinning	5-100 ppm	RT	0.59@50ppm	4 s/5 min	[38]
Co_3O_4/polyethyleneimine-CNT	Hydrothermal- method	1-1000 ppm	RT	70.9%@1000ppm	8/-	[39]
***p*-Co_3O_4 -CNFs**	Ultrasonication	0.5 – 5 ppm	RT	0.4 @ 0.5 ppm	4/6	Present work

ppb of NH_3 gas for *p*-Co_3O_4 supported heterojunction carbon fibers compared to pure Co_3O_4 NPs. Similarly, it shows rapid response time ($t_{res\ (90)}$) of 5-6 s for heterojunction materials than the pristine Co_3O_4 ($t_{res\ (90)}$: 12-14s). While increasing the concentrations of NH_3, the response and recovery characteristics were slower whereas, at trace level concentrations, time taken for response and recovery was much faster owing to the accessibility of minimal gas species to the sensor material as depicted from the Figure 5(C&F).

Moreover, the sensor responses were studied towards exposure to various interfering reducing gases, such as H_2S, isoprene, ethanol, acetone, etc. by keeping the concentration as 1 ppm constant for all gases in order to study the cross-interference properties. *p*-Co_3O_4 supported heterojunction carbon nano-fibers shows good selectivity towards NH_3 at room temperature which is depicted in Figure 6(A). Furthermore, the effect of humidity on the gas sensing performance of *p*-Co_3O_4 supported heterojunction carbon nano-fibers were studied as shown in Figure 6(B). The response was found to be dropped when the humidity exceeded 25% due to more RH % intervention of moisture persists on the material which decreased the electron transfer process at room temperature.

Table 1 compares the performance of *p*-Co_3O_4 supported heterojunction carbon nano-fibers based NH_3 gas sensors reported in literature.

The detection mechanism based on the sensing behavior of *p*-Co_3O_4 supported heterojunction carbon nano-fibers towards NH_3 gas can be elucidated in terms of their electron transport phenomenon. The as synthesized Co_3O_4 nanoparticles is being *p*-type conductivity and the carbon nanofibers behave like semi-metal nature, the electron received from the reducing gas NH_3 during the surface adsorption, these electrons could trap by the *p*-Co_3O_4 nanoparticles further transfer to one dimensional carbon nanofibers by reducing the charge carrier holes as depicted in the

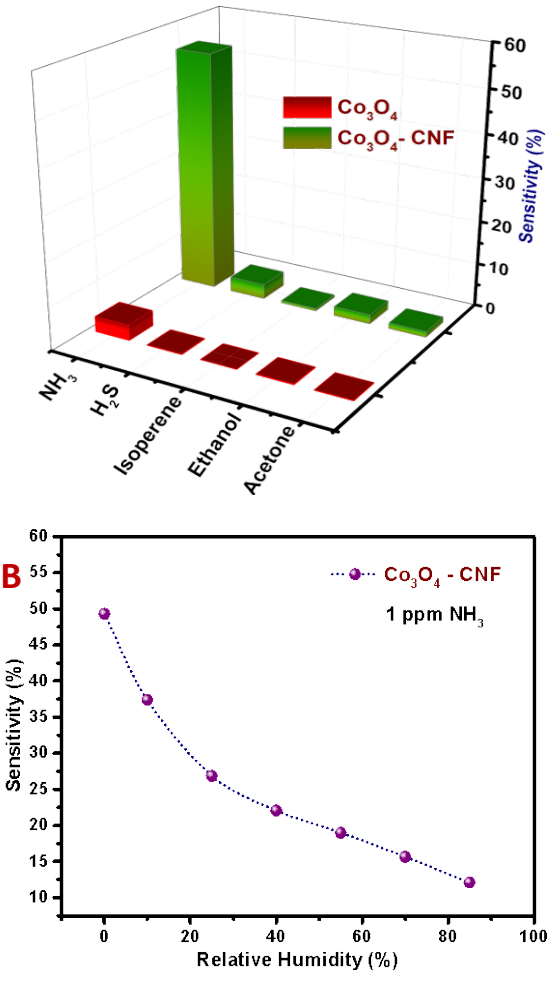

Figure 6(A) Cross-selectivity studies and **(B)** relative humidity interference studies of *p*-Co_3O_4 supported heterojunction carbon nano-fibers

schematic diagram in scheme 2. Consequently, a drastic increase in the sensor resistance was observed for the nanocomposite material. Owing to its dimensionality effect, the enhanced charge transport leads to boost the sensing performance of the nanocomposite heterojunction material. [35]

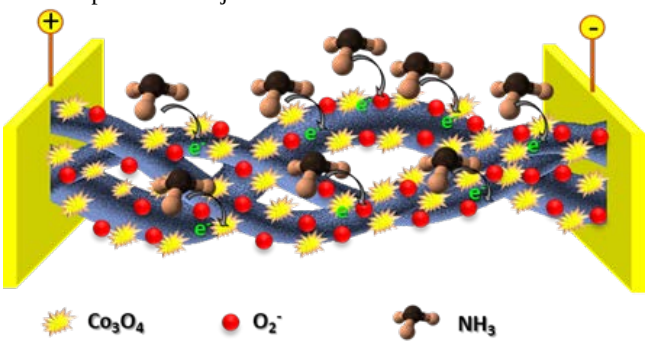

Scheme 2. Schematic representation of charge transport in *p*-Co_3O_4 supported heterojunction carbon nano-fibers during NH_3 adsorption

Conclusions

To summarize, *p*-Co_3O_4 supported heterojunction carbon fibers were synthesized by a simply ultrasonication process. The structural and morphological analysis of the *p*-Co_3O_4 supported heterojunction carbon nano-fibers was done by XRD, Raman spectroscopy and SEM characterizations to confirm the formation of heterojunctions. NH_3 gas sensing properties of *p*-Co_3O_4 supported heterojunction carbon nano-fibers based sensors exposed better sensitivity towards NH_3 in the range of 0.5–5 ppm with low detection limit of 500 ppb with rapid response of 5-6 s than that of sensitivity of pristine Co_3O_4 with response time ($t_{res(90)}$) of 12-14 s. The enhanced sensitivity towards NH_3 gas was attributed to the presence of carbon nanofiber further leads to fast charge transport mechanism. The present investigation discloses the importance of Co_3O_4 supported heterojunction carbon nano-fibers based sensor for cost-effective and room temperature sensing of NH_3 in the real-time applications.

Acknowledgments

The Authors wish to acknowledge the facilities and support provided by the management, PSG Sons and Charities, Coimbatore.

Conflict of Interest

Authors declared no conflict of interest.

Supplementary Information

Characterization techniques used, Schematic diagram, EDX spectra and table of NH_3 sensing properties.

References and Notes

1. B. Timmer, W. Olthuis, A. Van Den Berg. Ammonia sensors and their applications - A review. *Sensors Actuators, B Chem.* **2005**, 107 (2), 666–677.
2. V.P. Anju, P.R. Jithesh, S.K. Narayanankutty. A novel humidity and ammonia sensor based on nanofibers/polyaniline/polyvinyl alcohol. *Sensors Actuators, A Phys.* **2019**, 285, 35–44.
3. S. Crolius, D.G. Pugh, S. Morris, A. Valera-Medina. Safety Aspects; Elsevier Inc., **2021**.
4. A.S. GARDE. LPG and NH3 Sensing Properties of SnO2 Thick Film Resistors Prepared by Screen Printing Technique. *Sensors Transducers J.* **2010**, 122 (11), 128–142.
5. M.S. Abdelrahman, T.A. Khattab, A. Aldalbahi, M.R. Hatshan, M.E. El-Naggar. Facile development of microporous cellulose acetate xerogel immobilized with hydrazone probe for real time vapochromic detection of toxic ammonia. *J. Environ. Chem. Eng.* **2020**, 8 (6), 104573.
6. Z. Bielecki, T. Stacewicz, J. Smulko, J. Wojtas. Ammonia gas sensors: Comparison of solid-state and optical methods. *Appl. Sci.* **2020**, 10 (15).
7. Q. Qi, P.P. Wang, J. Zhao, et al. SnO2 nanoparticle-coated In2O3 nanofibers with improved NH3 sensing properties. *Sensors Actuators, B Chem.* **2014**, 194, 440–446.
8. P. Nakarungsee, S. Srirattanapibul, C. Issro, I.M. Tang, S. Thongmee. High performance Cr doped ZnO by UV for NH3 gas sensor. *Sensors Actuators, A Phys.* **2020**, 314, 112230.
9. T. Ahamad, M. Naushad, S.M. Alshheri. Fabrication of highly porous N/S doped carbon embedded with CuO/CuS nanoparticles for NH3 gas sensing. *Mater. Lett.* **2020**, 268, 127515.
10. H.I. Chen, C.Y. Hsiao, W.C. Chen, et al. Characteristics of a Pt/NiO thin film-based ammonia gas sensor. *Sensors Actuators, B Chem.* **2018**, 256, 962–967.
11. Z. Li, Z. Lin, N. Wang, et al. High precision NH3 sensing using network nano-sheet Co3O4 arrays based sensor at room temperature. *Sensors Actuators, B Chem.* **2016**, 235, 222–231.
12. B. Saruhan, R. Lontio Fomekong, S. Nahirniak. Review: Influences of Semiconductor Metal Oxide Properties on Gas Sensing Characteristics. *Front. Sensors* **2021**, 2 (April), 1–24.
13. J. Zhang, Z. Qin, D. Zeng, C. Xie. Metal-oxide-semiconductor based gas sensors: Screening, preparation, and integration. *Phys. Chem. Chem. Phys.* **2017**, 19 (9), 6313–6329.
14. Z. Li, H. Li, Z. Wu, et al. Advances in designs and mechanisms of semiconducting metal oxide nanostructures for high-precision gas sensors operated at room temperature. *Mater. Horizons* **2019**, 6 (3), 470–506.
15. M.S. Chavali, M.P. Nikolova. Metal oxide nanoparticles and their applications in nanotechnology. *SN Appl. Sci.* **2019**, 1 (6), 1–30.
16. Y. Cai, J. Xu, Y. Guo, J. Liu. Ultrathin, Polycrystalline, Two-Dimensional Co 3 O 4 for Low-Temperature CO Oxidation. *ACS Catal.* **2019**, 9 (3), 2558–2567.
17. C.S. Jincy, P. Meena. Synthesis, characterization, and NH3 gas sensing application of Zn doped cobalt oxide nanoparticles. *Inorg. Chem. Commun.* **2020**, 120 (May), 108145.
18. H. Xie, G. Luo, Y. Niu, et al. Synthesis and utilization of Co3O4 doped carbon nanofiber for fabrication of hemoglobin-based electrochemical sensor. *Mater. Sci. Eng. C* **2020**, 107 (March 2019), 110209.
19. Y. Shi, X. Pan, B. Li, M. Zhao, H. Pang. Co3O4 and its composites for high-performance Li-ion batteries. *Chem. Eng. J.* **2018**, 343 (March), 427–446.
20. Z. Wang, S. Wu, J. Wang, A. Yu, G. Wei. Carbon nanofiber-based functional nanomaterials for sensor applications. *Nanomaterials* **2019**, 9 (7).
21. Kenry, C.T. Lim. Nanofiber technology: current status and emerging developments. *Prog. Polym. Sci.* **2017**, 70, 1–17.
22. S. Abouali, M. Akbari Garakani, B. Zhang, et al. Co3O4/porous electrospun carbon nanofibers as anodes for high performance Li-ion batteries. *J. Mater. Chem. A* **2014**, 2 (40), 16939–16944.
23. G.H. An, H.J. Ahn. Carbon nanofiber/cobalt oxide nanopyramid core-shell nanowires for high-performance lithium-ion batteries. *J. Power Sources* **2014**, 272, 828–836.
24. B. Geng, F. Zhan, C. Fang, N. Yu. A facile coordination compound precursor route to controlled synthesis of Co3O4 nanostructures and their room-temperature gas sensing properties. *J. Mater. Chem.* **2008**, 18 (41), 4977–4984.
25. B. Geng, F. Zhan, H. Jiang, Z. Xing, C. Fang. Facile production of self-assembly hierarchical dumbbell-like CoOOH nanostructures and their room-temperature CO-gas-sensing properties. *Cryst. Growth Des.* **2008**, 8 (10), 3497–3500.
26. K.G. Nair, V. Ramakrishnan, R. Unnathpadi, K.K. Karuppanan, B. Pullithadathil. Unraveling Hydrogen Adsorption Kinetics of Bimetallic Au-Pt Nanoisland-Functionalized Carbon Nanofibers for Room-Temperature Gas Sensor Applications. *J. Phys. Chem. C* **2020**, 124 (13), 7144–7155.

27. A. Aljabour. Long-Lasting Electrospun Co3O4 Nanofibers for Electrocatalytic Oxygen Evolution Reaction. *ChemistrySelect* **2020**, 5 (25), 7482–7487.
28. K.G. Nair, R. Vishnuraj, B. Pullithadathil. Highly Sensitive, Flexible H2 Gas Sensors Based on Less Platinum Bimetallic Ni-Pt Nanocatalyst-Functionalized Carbon Nanofibers. *ACS Appl. Electron. Mater.* **2021**, 3 (4), 1621–1633.
29. V.A. Online. RSC Advances E ff ect of graphene incorporation in carbon nano fi ber decorated with TiO 2 for photoanode. **2017**, 6574–6582.
30. L. Daza-gómez, V. Ruiz-ruiz, J.A. Mendoza-nieto, H. Pfei, D. Díaz. Applied Clay Science Co 3 O 4 nanostructures and Co 3 O 4 supported on halloysite nanotubes : New highly active and thermally stable feasible catalysts for CO oxidation. **2020**, 190 (April).
31. Y. Meng, G. Wang, M. Xiao, et al. materials Ionic liquid-derived Co 3 O 4 / carbon nano-onions composite and its enhanced performance as anode for lithium-ion batteries. *J. Mater. Sci.* **2017**.
32. H. Wang, J. Zhou, J. Sun, et al. Hierarchically Flower-Like Cobalt Oxide @ Doped-Sn Carbon Nanofiber with Core-Shell structure as Anodes for Lithium Ion Battery. **2020**, d, 9849–9863.
33. J. Zhou, J. Zhang, A.U. Rehman, et al. Synthesis , characterization , and ammonia gas sensing properties of Co 3 O 4 @ CuO nanochains. **2017**, 3757–3770.
34. S.J.Y.Z.D. Lin. Ammonia gas sensors with Au-decorated carbon nanotubes. *Microsyst. Technol.* **2018**, 3456789, 1–4.
35. U. Latif, F.L. Dickert. Graphene Hybrid Materials in Gas Sensing Applications †. **2015**, No. September, 30504–30524.
36. J. Deng, R. Zhang, L. Wang, Z. Lou, T. Zhang. Sensors and Actuators B : Chemical Enhanced sensing performance of the Co 3 O 4 hierarchical nanorods to NH 3 gas. *Sensors Actuators B. Chem.* **2015**, 209, 449–455.
37. L. Wang, Z. Lou, R. Zhang, et al. Hybrid Co3O4/SnO2 Core-Shell Nanospheres as Real-Time Rapid-Response Sensors for Ammonia Gas. *ACS Appl. Mater. Interfaces* **2016**, 8 (10), 6539–6545.
38. Q. Feng, X. Li, J. Wang, A.M. Gaskov. Reduced graphene oxide (rGO) encapsulated Co3O4 composite nanofibers for highly selective ammonia sensors. *Sensors Actuators, B Chem.* **2016**, 222, 864–870.
39. Y. Lin, K. Kan, W. Song, et al. Controllable synthesis of Co3O4/polyethyleneimine-carbon nanotubes nanocomposites for CO and NH3 gas sensing at room temperature. *J. Alloys Compd.* **2015**, 639, 187–196.